Contents lists available at UGC-CARE

International Journal of Pharmaceutical Sciences and Drug Research

[ISSN: 0975-248X; CODEN (USA): IJPSPP]

journal home page : http://ijpsdr.com/index.php/ijpsdr

Research Article

Molecular Docking, Binding Energy and Molecular Dynamics Simulation Studies of Piperazin-1-ylpyridazine Derivatives as Deoxycytidine Triphosphate Pyrophosphatase Inhibitors

Shashank S. Mishra, Chandra S. Sharma*

Department of Pharmaceutical chemistry, Faculty of Pharmacy, Bhupal Nobles' University, Udaipur-313001, Rajasthan, India

ARTICLE INFO

Article history:

Received: 02 April, 2021

Revised: 08 February, 2022

Accepted: 19 February, 2022

Published: 30 March, 2022

Keywords:

Binding energy calculation,
dCTPase enzyme,
Molecular docking,
Molecular dynamics.

DOI:

10.25004/IJPSDR.2022.140203

ABSTRACT

Cancer is a most serious health problem globally due to increased mortality. Deoxycytidine triphosphate pyrophosphatase (dCTPase) enzyme involved in cancer progression and cancer cell stemness and found over-expressed in breast cancer. This overexpression makes it of attractive target to discover new class of anticancer therapy. In the present work, we have selected piperazin-1-ylpyridazine derivatives as dCTPase inhibitors and performed molecular docking and dynamics simulations analysis to evaluate the binding pattern of selected compounds with target protein. Compound P21 has highest binding affinity towards dCTPase protein with -4.649 as Glide Gscore. In all compounds, only pyridazine and caboxamide nucleus involves in hydrogen bond formation and benzyl or phenyl nucleus involves in π-π stacking interaction. These observations provide the valuable lead for ligand based anticancer drug design.

Introduction

Cancer is one of the major public health diseases worldwide with a high mortality rate. The development of cancer relies upon the mutations or alterations emerging inside the cell, driving aberrant behaviour that can sidestep the distinctive checkpoints essential for normal cell health.[1] Alteration in cellular metabolism through mutations or expression changes in tumor suppressor genes and oncogenes serve as fuel to cancer progression.[2] Therefore, the accumulation of genetic mutational changes contributes to cancer cell growth. In various treatment approaches, the use of synthetic nucleoside and nucleobase analogs are important strategy due to interruption in genome integrity and nucleotide homeostasis.[3] In anti-metabolites, nucleosides analogues are effective anticancer drugs exert their effect by inhibiting cell proliferation.

The dCTP pyrophosphatase 1 (dCTPase) enzyme is also known as DCTPP1 and XTP3-transactivated protein A (XTP3TPA).[4-6] The dCTPase enzyme can also hydrolyze C5-modified dNTPs such as 5-methyl, 5-halogenated and 5-formyl deoxycytidines, and along with additional 'house-cleaning' function.[4] Various research investigations suggest that dCTPase is associated with cancer progression, cancer cell stemness, association with poor clinical prognosis and decreased response to anticancer nucleoside analogues.[5-9] Song et al also reported that the dCTPase enzyme was significantly over-expressed in breast cancer and found its strong contribution with tumor progression and poor prognosis

***Corresponding Author:** Author Name

Address: Department of Pharmaceutical chemistry, Faculty of Pharmacy, Bhupal Nobles' University, Udaipur-313001, Rajasthan, India

Email ✉**:** cssmedchem@gmail.com

Tel.: +91-9828173650

Relevant conflicts of interest/financial disclosures: The authors declare that the research was conducted in the absence of any commercial or financial relationships that could be construed as a potential conflict of interest.

in breast cancer.[7] This contribution of dCTPase in carcinogenesis and nucleotide homeostasis makes it of great interest to further elucidate the cellular function of this all-α NTP pyrophosphatase family member. There are only few dCTPase inhibitors reported but no one can become drug.

The objective of the present investigation is to identify the binding mechanism through molecular docking, molecular dynamics simulation and binding energy studies. To the best of our knowledge, there is no one work has been reported on the molecular modelling studies of dCTPase inhibitors.

Materials and Methods

Selection of Data Sets

The series of 26 piperazin-1-ylpyridazine derivatives were selected for the study.[10]

Homology Modelling and Model Validation

Homology modelling approach was used for determining 3D structure of dCTPase enzyme as no PDB structure was available in the Protein Data Bank. The target amino acid sequence file of dCTPase (PDB code: 2OIG) was retrieved from UniProt. Template search with Blast[11] and HHBlits[12] has been performed against the Swiss-Model template library. The template 2A3Q was selected on the basis of sequence identities having 100% with the queried protein and quaternary structure quality estimate (QSQE) as 0.66. The QSQE score is a number between 0 and 1, reflecting the expected accuracy of the interchain contacts for a model built based a given alignment and template. Homology model of dCTPase was built based on the target-template alignment using ProMod3. Coordinates which are conserved between the target and the template are copied from the template to the model. The quality of the model was estimated using the Qualitative model energy analysis (QMEAN) scoring function and Global model quality estimation (GMQE) score. Further obtained homology model was validated by molecular dynamics simulations calculations. The validated homology model by molecular dynamics was shown in Fig. 1.

Active Site Identification

The putative active site of dCTPase modelled protein was identified by using SiteMap. A SiteMap calculation begins with an initial search stage that determines one or more regions on or near the protein surface, called sites that may be suitable for binding of a ligand to the receptor. The search uses a grid of points, called site points, to locate the sites. In the second stage, contour maps (site maps) are generated, producing hydrophobic and hydrophilic maps. The hydrophilic maps are further divided into donor, acceptor, and metal-binding regions. The evaluation stage, which concludes the calculation, assesses each site by calculating various properties.[13,14]

Receptor Grid Generation and Molecular Docking

The identified putative site was selected for receptor grid generation by using glide module of Maestro.[15] For, molecular docking analysis, ligands were prepared using ligprep tool of Maestro. Epic was used to generate tautomers and generate low energy ring conformation for each ligand with default settings. Further, glide docking was executed in extra precision (XP) mode. The docking calculations were accomplished by using OPLS_2005 force field. The protein was set as rigid while ligands were select as flexible for docking analysis.

Binding Free Energy Calculations

Prime molecular mechanics with generalised Born and surface area solvation (MM-GBSA) is a tool of Schrödinger software which was used to calculate relative binding energies of all docked protein-ligand complexes with default parameters.[16] Prime MM-GBSA free energy is calculated by given equation.[17]

$$\Delta G_{bind} = G_{complex} - (G_{protein} + G_{ligand})$$

Where ΔG_{bind} is the binding free energy, $G_{complex}$ is free energy of complex, $G_{protein}$ and G_{ligand} is free energy of the target protein and ligand, respectively.

Molecular Dynamics Simulations

Molecular dynamics simulations were carried out through Desmond tool of Schrödinger software in order to assert the stability and conformation of dCTPase inhibitor complex.[18] From all analysed compounds, the best compounds were selected for simulation study on the basis of glide score parameters, binding energy, number of hydrogen bonds and dCTPase inhibitory activity. We selected compound P14 and P21 for MD

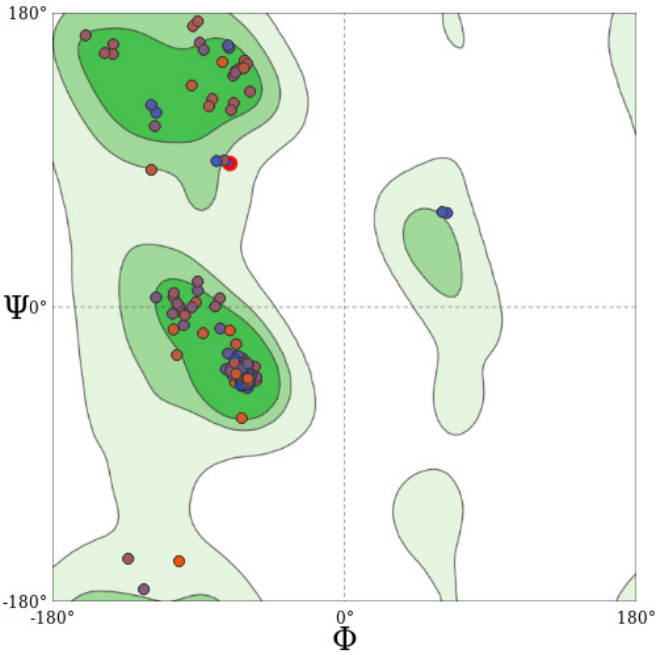

Fig. 1: Ramachandran plot of dCTPase modelled protein

simulations. Selected complex was solvated by selecting 1-palmitoyl-2-oleoyl-sn-glycero-3-phosphocholine (POPC) as membrane; SPC as solvent model and orthorhombic box shaped periodic boundary conditions selected and furthermore calculated the volume of the selected box. For neutralization of the solvated system, the required number of ions was added and the salt concentration was set at 0.15 M of Na^+ and Cl^- ions to simulate the background salt and physiological conditions. Energy minimization of complex was done by maximum 2000 iterations to remove steric clashes. The energy minimized system was subjected for continuing heating from 0 to 300 K for 20 ns with constant volume. NPT ensemble was selected by considering 300 K temperature and 1.01325 bar as pressure.[19] The model system was relaxed; hence, 20 ns simulations were performed and trajectory was recorded at 4.8 picoseconds. The protein-ligand root mean square deviation (RMSD), root mean square fluctuation (RMSF), contacts and ligand properties were investigated to check the conformational behaviour and stability of the simulated complex during the 20 ns simulations.

Results and Discussion

Homology Modelling and Validation of Protein

To rationalize the observed QSAR, we determined the 3D structure of dCTPase enzyme through homology modelling approach. The target sequence file 2OIG and the template 2A3Q were selected to build homology model using target-template alignment. GMQE is a quality estimation which combines properties from the target–template alignment and the template search method. QMEAN score is a composite estimator based on different geometrical properties and provides both global (i.e., for the entire structure) and local (i.e., per residue) absolute quality estimates on the basis of one single model. The obtained model having the GMQE score 0.67 and the QMEAN score 0.62 indicates the higher reliability and accuracy of the model. The modelled protein has four chains and the QMEAN Z-score plot is shown in Fig. 2, which provides an estimate of the "degree of nativeness" of the structural features observed in the modelled protein on a global scale. QMEAN Z-scores around zero indicate good agreement between the model structure and experimental structures of similar size.[20]

The geometry optimization of the modelled protein has been done through molecular dynamics simulations which indicate the RMSD score 2.2 Å and RMSF score 1.5 Å (Fig. 3). The optimal range 1–3 Å are perfectly acceptable for small, globular proteins. Hence, the model shows stable nature of protein architecture.

Active Site Identification

For generating the binding site, extensive search was accomplished by SiteMap. It results multiple sites which are tabulated in Table 1.

The Site score is based on a weighted sum of several of the properties that are number of site points, enclosure score and hydrophilic score. With Site score of 0.987 and D score of 0.898, site 1 was selected for molecular docking and dynamics calculation studies (Fig. 4).

Molecular Docking and Binding Free Energy Calculations

To rationalize the scope of investigation, we performed molecular docking studies of all compounds with

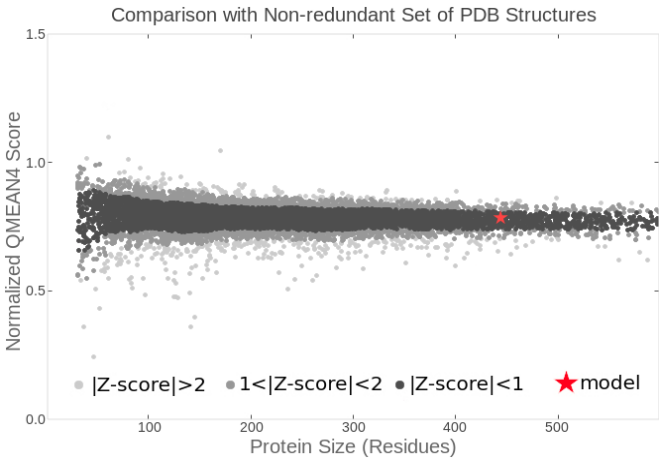

Fig. 2: The QMEAN Z-score plot of obtained homology modelled protein.

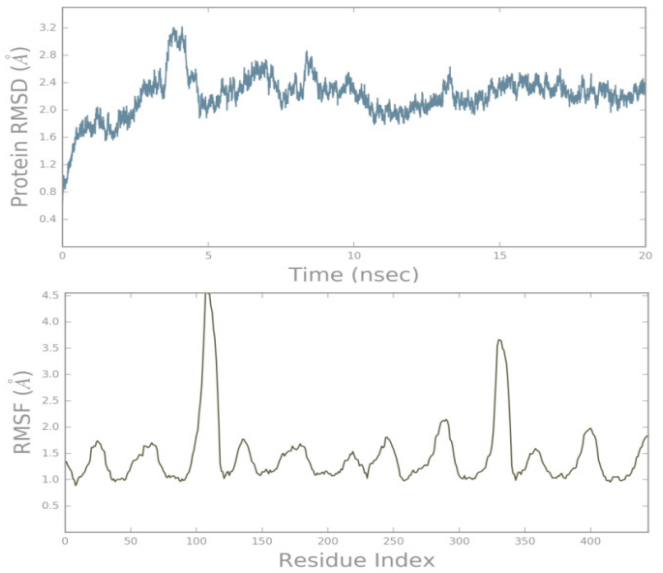

Fig. 3: Molecular dynamics simulation results for dCTPase modelled protein.

Table 1: Identified active sites and site score predicted by SiteMap.

Site number	*Site score*	*D score*	*Volume*
Site 1	0.987	0.898	207.858
Site 2	0.986	0.954	171.157
Site 3	0.946	0.886	166.012
Site 4	0.807	0.770	128.625
Site 5	0.781	0.746	126.224

modelled protein of dCTPase enzyme. The receptor grid was generated around the identified active site of the protein, prior to docking. The molecular docking results with binding free energy calculations were depicted in Tables 2 and 3. Pharmacokinetic parameters calculations were performed by using Molinspiration online server. The results are tabulated in Table 3.

Compound P21 (*N*-benzyl-1-(6-(4-(o-tolylsulfonyl) piperazin-1-yl)pyridazin-3-yl)methanamine) has highest binding affinity towards dCTPase protein with -4.649 as Glide Gscore. It shows two hydrogen bonds with residues Gln82 (sidechain) and Glu78 (backbone). The pyridazine ring of compound P21 forms π-π stacking interaction with Arg109 residue. The amino acid residues involved in hydrophobic interaction with compound P21 are Ala108, Phe23, Trp47, Pro79, Trp84, Phe71, Pro81 and pro53 (Fig. 5).

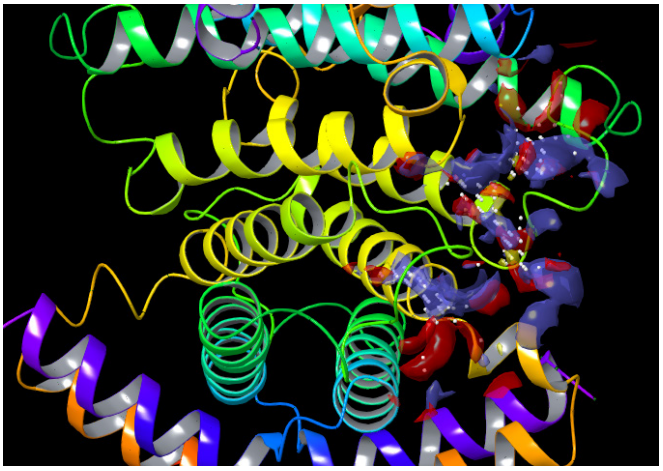

Fig. 4: Identified active site in dCTPase protein.

Table 2: Chemical structure and docking results of piperazine derivatives

Com. no.	*Structure*	*Glide gscore*	*No. of hydrogen bond*	*H-bond interaction*
P1	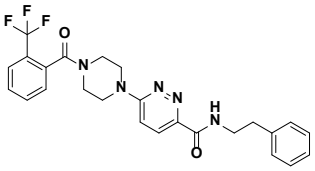	-3.224	03	Gly80, Arg109, Asp76
P2	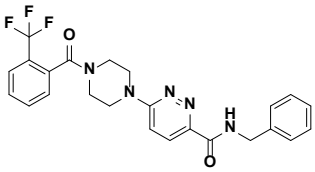	-3.628	03	Gly80, Arg109, Asp76
P3	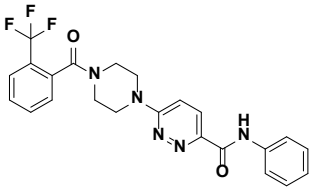	-3.490	02	Arg109, Glu78
P4	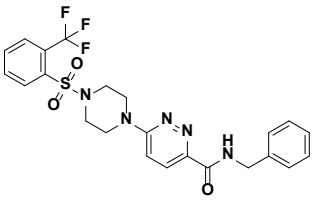	-3.648	03	Gly80, Arg109, Asp76
P5	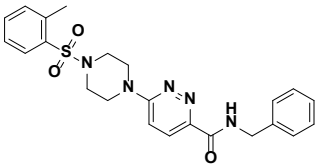	-3.453	03	Gly80, Arg109, Asp76
P6	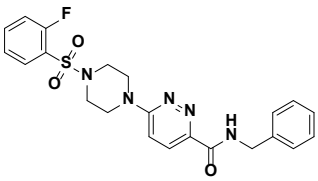	-3.232	03	Gly80, Arg109, Asp76

Cont...

Com. no.	*Structure*	*Glide gscore*	*No. of hydrogen bond*	*H-bond interaction*
P7	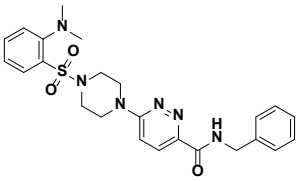	-3.630	03	Gly80, Arg109, Asp76
P8	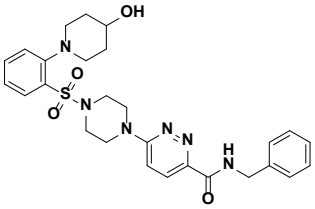	-3.542	03	Gly80, Arg109, Asp76
P9	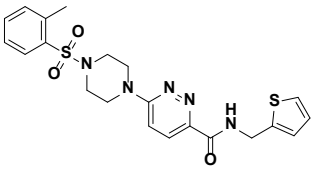	-3.339	03	Gly80, Arg109, Asp76
P10	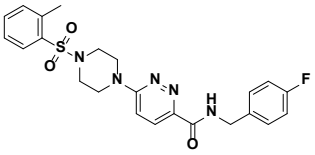	-3.588	03	Gly80, Arg109, Asp76
P11	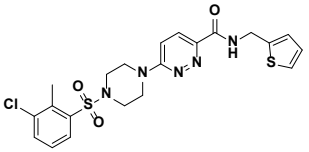	-3.922	03	Gly80, Arg109, Asp76
P12	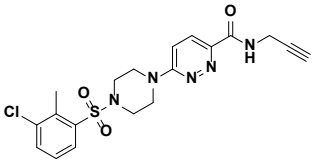	-2.466	01	Asp76
P13	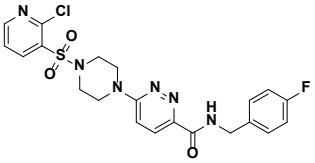	-3.280	02	Asp76, Arg109
P14	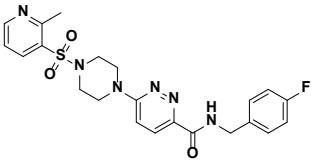	-3.469	03	Asp76, Arg109
P15	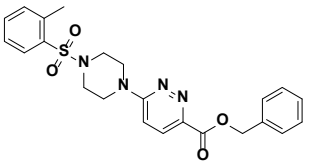	-2.430	02	Arg109, Gln82

Cont...

Com. no.	*Structure*	*Glide gscore*	*No. of hydrogen bond*	*H-bond interaction*
P16	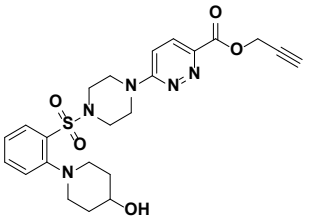	-2.253	03	Arg109, His51, Gln52
P17	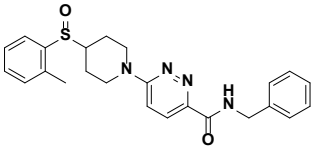	-3.370	03	Gly80, Arg109, Asp76
P18	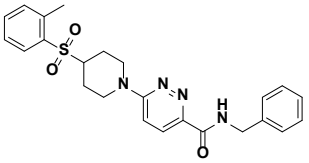	-3.063	02	Arg109, Asp76
P19	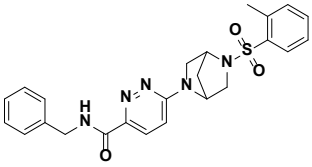	-3.246	03	Gly80, Arg109, Asp76
P20	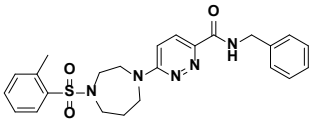	-3.234	03	Arg109, Asp76
P21	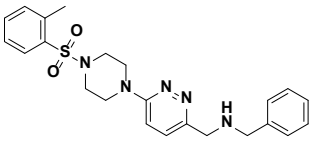	-4.649	02	Gln82, Glu78
P22	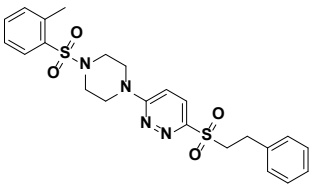	-2.211	-	-
P23	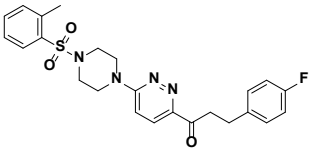	-2.499	02	Arg109, Gln52
P24	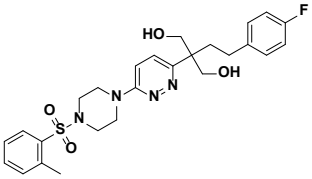	-2.545	03	Glu48, Thr77

Cont...

Com. no.	*Structure*	*Glide gscore*	*No. of hydrogen bond*	*H-bond interaction*
P25	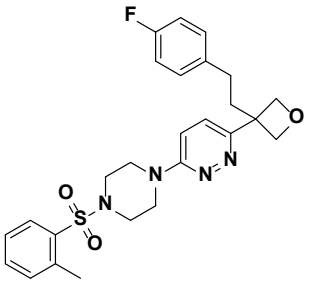	-1.439	01	Gly80
P26	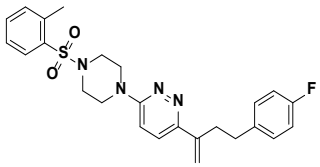	-2.540	01	Thr77

Table 3: Binding energies and pharmacokinetic parameters calculations of piperazine derivatives

Com. no.	*dG Bind*	*dG bind coulomb*	*dG bind lipo*	*LogP*	*TPSA*	*Volume*	*M. W.*
P1	-51.430	-31.416	-30.214	3.00	78.43	415.75	483.49
P2	-59.993	-41.129	-26.716	2.59	78.43	398.95	469.47
P3	-51.761	-22.819	-26.964	2.89	78.43	382.15	455.44
P4	-62.180	-11.572	-26.351	2.94	95.50	411.40	505.52
P5	-61.524	-13.393	-26.392	2.49	95.50	396.66	451.55
P6	-61.333	-14.104	-26.340	2.21	95.50	385.03	455.51
P7	-61.287	-13.458	-26.368	2.15	98.74	426.01	480.59
P8	-65.407	-16.101	-32.396	1.17	118.97	474.10	536.66
P9	-62.229	-7.204	-29.194	2.39	95.50	387.37	457.58
P10	-60.232	-14.101	-26.112	2.66	95.50	401.59	469.54
P11	-70.287	-12.082	-30.414	3.02	95.50	400.91	492.03
P12	-43.833	7.327	-22.082	1.89	95.50	361.05	433.92
P13	-45.628	-6.991	-26.951	1.99	108.39	394.41	490.95
P14	-48.531	-6.853	-25.279	1.41	108.39	397.44	470.53
P15	-53.428	4.714	-26.696	3.33	92.71	393.24	452.54
P16	-26.505	13.616	-15.783	0.57	116.17	421.53	485.57
P17	-56.992	-38.382	-26.869	2.55	75.19	394.95	434.56
P18	-45.969	-20.063	-26.909	3.02	92.26	400.70	450.26
P19	-64.404	-15.424	-27.789	2.60	95.50	402.67	463.56
P20	-47.946	-2.260	-26.780	2.76	95.50	413.46	465.58
P21	-42.576	-96.798	-24.628	2.86	78.43	394.48	437.57
P22	-45.748	25.044	-29.810	3.45	100.54	413.51	486.62
P23	-44.520	15.021	-26.547	3.91	83.47	405.99	468.55
P24	-34.899	9.464	-21.964	3.16	106.86	453.15	514.62
P25	-37.138	15.084	-31.450	4.27	75.64	435.26	496.61
P26	-39.271	17.236	-24.333	4.74	66.40	414.74	466.58

All compounds show excellent binding affinity with target protein in terms of Glide Gscore. Except compound P22, all compounds show hydrogen bond interactions with different amino acid residues. Compound P14 (*N*-(4-fluorobenzyl)-6-(4-((2-methylpyridin-3-yl)sulfonyl) piperazin-1-yl)pyridazine-3-carboxamide) also exhibit

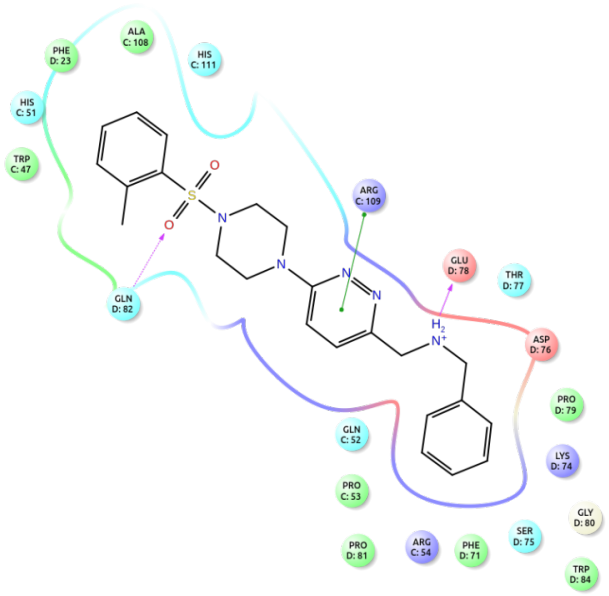

Fig. 5: Protein-ligand interaction diagram of compound P21.

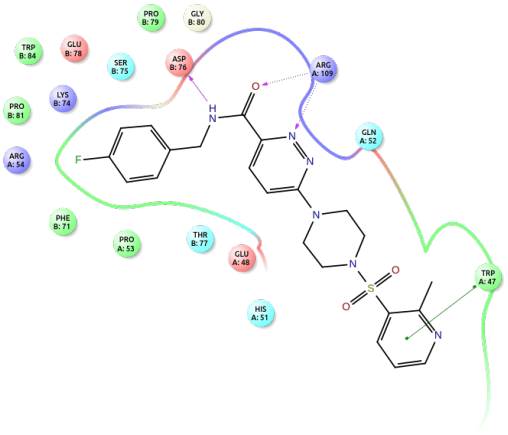

Fig. 6: Protein-ligand interaction diagram of compound P14.

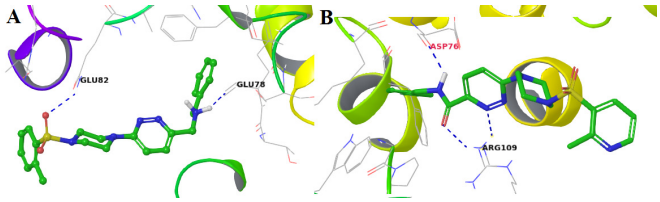

Fig. 7: Binding mode of docked target protein and **A.** Compound P21 and **B.** Compound P14.

-3.469 Glide Gscore and good vdW contacts. The compound P14 has tightly fixed in binding pocket due to formation of hydrogen bond with residues Asp76 (backbone), Arg109 (sidechain) and π-π stacking interaction with Trp47 (Fig. 6). The interesting fact is that in many compounds, only pyridazine and caboxamide nucleus involves in hydrogen bond formation and benzyl or phenyl nucleus involves in π-π stacking interaction. Most of the compounds bind with target protein in a similar way.

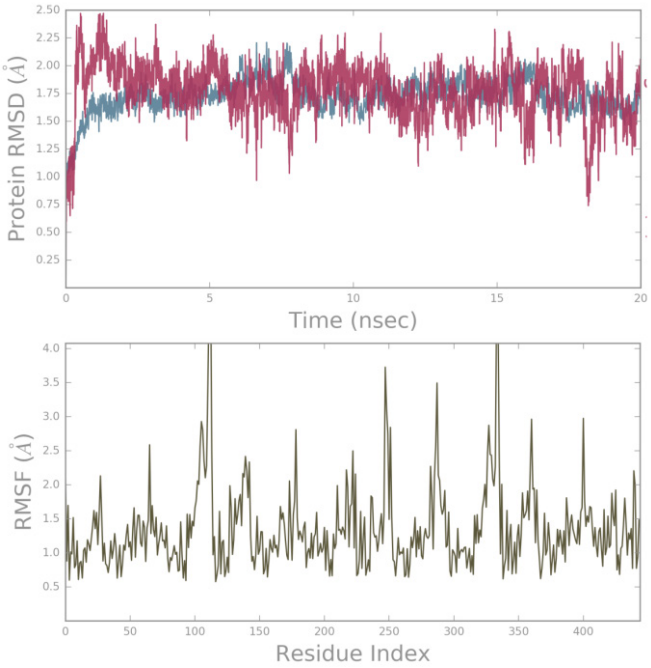

Fig. 8: RMSD and RMSF plot of compound P14.

Docking results revealed that the target protein has large binding cavity which is consists of hydrophobic pocket (Ala108, Phe23, Pro79, Phe71, Pro81, Pro53, Trp47, Trp84), hydrogen bonding site (Gly80, Arg109, Asp76, Glu48, Thr77) and other interactions (Fig. 7). The hydrophobic interactions enhance the binding affinity.[21] Hence, the presence of sulfonamide, carboxamide connected with left side piperazine nucleus contribute in binding as well as in activity. The pyridazine ring with carboxamide moiety connected with right side piperazine nucleus enhances the binding affinity. The presence of benzyl ring with carboxamide moiety (right side) plays a wider role in π-π stacking interaction and salt bridge formation.

Molecular dynamics simulations

Molecular dynamics allows the atomic-level characterization of various bimolecular processes such as analysis of stability of protein-ligands interactions associated with activation and deactivation of various molecular pathways.[22] In this study, the simulations were performed on compound P14 and P21 by solvated and energy minimized system. The functional nature of the complex is based upon their movement and folding of backbone inside the simulated system. The RMSD plot of protein shows the structural changes in backbone, Cα and side chain amino acid residues of the dCTPase protein throughout the 20 ns simulation. The RMSD of compound P14 and P21 for 20 ns was found to be 1.75 Å and 1.50 Å respectively which indicates changes are perfectly acceptable for small, globular proteins (Figs. 8 and 9). The plot shows compound P14 and P21 was perfectly aligned on the protein backbone and then the RMSD was calculated

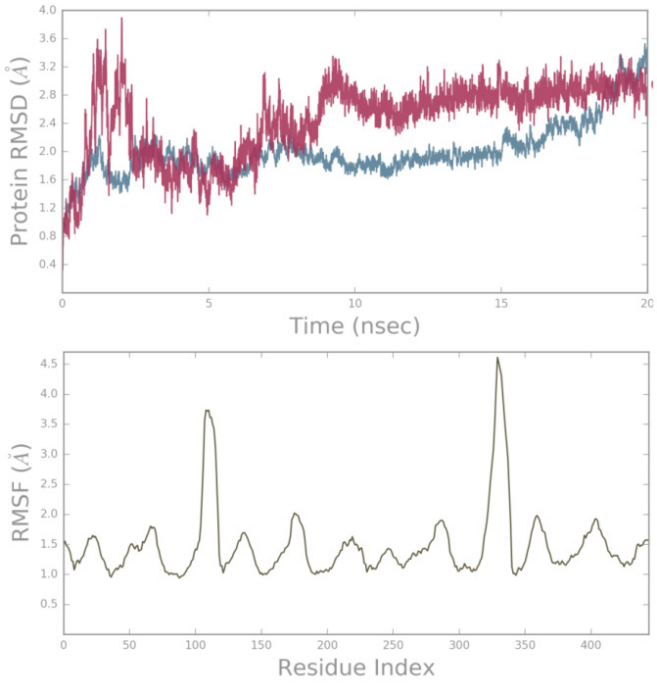

Fig. 9: RMSD and RMSF plot of compound P21.

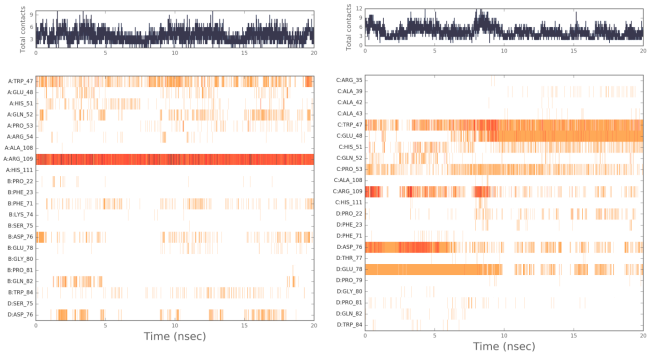

Fig. 10: Observed protein-ligand contacts of docked compound P14 and P21.

which indicates excellent binding with the binding site of protein.

The RMSF of compound P14 and P21 was found to be 1.5 Å and 1.3 Å respectively which indicates N and C-terminal fluctuate more than any other part of the protein (Figs. 8 and 9). The different protein-ligand contacts were observed which is utilized for design of the novel inhibitors with potent activity and selectivity (Fig. 10). The residues involved in hydrogen bond interactions are Arg109, Glu48, Asp76 and Trp47 shown strong influence on drug specificity, metabolism and adsorption.

Conclusion

The dCTPase enzyme involves in the catabolism of noncanonical and canonical nucleoside triphosphates. Owing to the role of dCTPase in cancer stemness and progression, dCTPase becomes an attractive target for anticancer drug discovery programme. To design selective and potent dCTPase inhibitors, it is necessary to investigate the inhibitor-protein binding pattern. In the present investigation, docking results demonstrate that all compounds show excellent binding affinity with target protein. We also executed molecular dynamics simulations to explore the binding mechanism. The simulation study suggests that all compounds binds in a similar way and the binding pocket consists of hydrophobic pocket (Ala108, Phe23, Pro79, Phe71, Pro81, Pro53, Trp47, Trp84), hydrogen bonding site (Gly80, Arg109, Asp76, Glu48, Thr77) and other interactions. Therefore, piperazin-1-ylpyridazines could be potent and novel class of dCTPase inhibitors for anticancer therapy. This research investigation can be providing the platform for drug design of potent and efficacious dCTPase inhibitors through the understanding of binding mechanism.

Acknowledgements

The authors are thankful to Dr. Sourav Kalra for providing computational facilities to accomplish this research work.

References

1. Vogelstein B, Papadopoulos N, Velculescu VE, Zhou S, Diaz LA, Kinzler KW. Cancer Genome Landscapes. Science [Internet]. American Association for the Advancement of Science (AAAS); 2013 Mar 28;339(6127):1546–58. Available from: http://dx.doi.org/10.1126/science.1235122
2. Counihan JL, Grossman EA, Nomura DK. Cancer Metabolism: Current Understanding and Therapies. Chemical Reviews [Internet]. American Chemical Society (ACS); 2018 Jun 25;118(14):6893–923. Available from: http://dx.doi.org/10.1021/acs.chemrev.7b00775
3. Jordheim LP, Durantel D, Zoulim F, Dumontet C. Advances in the development of nucleoside and nucleotide analogues for cancer and viral diseases. Nature Reviews Drug Discovery [Internet]. Springer Science and Business Media LLC; 2013 May 31;12(6):447–64. Available from: http://dx.doi.org/10.1038/nrd4010
4. Requena CE, Pérez-Moreno G, Ruiz-Pérez LM, Vidal AE, González-Pacanowska D. The NTP pyrophosphatase DCTPP1 contributes to the homoeostasis and cleansing of the dNTP pool in human cells. Biochemical Journal [Internet]. Portland Press Ltd.; 2014 Mar 14;459(1):171–80. Available from: http://dx.doi.org/10.1042/bj20130894
5. Vértessy BG, Tóth J. Keeping Uracil Out of DNA: Physiological Role, Structure and Catalytic Mechanism of dUTPases. Accounts of Chemical Research [Internet]. American Chemical Society (ACS); 2008 Oct 7;42(1):97–106. Available from: http://dx.doi.org/10.1021/ar800114w
6. Requena CE, Pérez-Moreno G, Horváth A, Vértessy BG, Ruiz-Pérez LM, González-Pacanowska D, et al. The nucleotidohydrolases DCTPP1 and dUTPase are involved in the cellular response to decitabine. Biochemical Journal [Internet]. Portland Press Ltd.; 2016 Aug 30;473(17):2635–43. Available from: http://dx.doi.org/10.1042/bcj20160302
7. Song F, Xia L, Ji P, Tang Y, Huang Z, Zhu L, et al. Human dCTP pyrophosphatase 1 promotes breast cancer cell growth and stemness through the modulation on 5-methyl-dCTP metabolism and global hypomethylation. Oncogenesis [Internet]. Springer Science and Business Media LLC; 2015 Jun;4(6):e159–e159. Available from: http://dx.doi.org/10.1038/oncsis.2015.10
8. Zhang Y, Ye WY, Wang JQ, Wang SJ, Ji P, Zhou GY, et al. dCTP pyrophosphohydrase exhibits nucleic accumulation in multiple carcinomas. European Journal of Histochemistry [Internet].

PAGEPress Publications; 2013 Sep 25;57(3):29. Available from: http://dx.doi.org/10.4081/ejh.2013.e29
9. Morisaki T, Yashiro M, Kakehashi A, Inagaki A, Kinoshita H, Fukuoka T, et al. Comparative Proteomics Analysis of Gastric Cancer Stem Cells. Hjelmeland AB, editor. PLoS ONE [Internet]. Public Library of Science (PLoS); 2014 Nov 7;9(11):e110736. Available from: http://dx.doi.org/10.1371/journal.pone.0110736
10. Llona-Minguez S, Höglund A, Ghassemian A, Desroses M, Calderón-Montaño JM, Burgos Morón E, et al. Piperazin-1-ylpyridazine Derivatives Are a Novel Class of Human dCTP Pyrophosphatase 1 Inhibitors. Journal of Medicinal Chemistry [Internet]. American Chemical Society (ACS); 2017 May 16;60(10):4279–92. Available from: http://dx.doi.org/10.1021/acs.jmedchem.7b00182
11. Camacho C, Coulouris G, Avagyan V, Ma N, Papadopoulos J, Bealer K, et al. BLAST+: architecture and applications. BMC Bioinformatics [Internet]. Springer Science and Business Media LLC; 2009 Dec;10(1). Available from: http://dx.doi.org/10.1186/1471-2105-10-421
12. Remmert M, Biegert A, Hauser A, Söding J. HHblits: lightning-fast iterative protein sequence searching by HMM-HMM alignment. Nature Methods [Internet]. Springer Science and Business Media LLC; 2011 Dec 25;9(2):173–5. Available from: http://dx.doi.org/10.1038/nmeth.1818
13. Halgren T. New Method for Fast and Accurate Binding-site Identification and Analysis. Chemical Biology & Drug Design [Internet]. Wiley; 2007 Feb;69(2):146–8. Available from: http://dx.doi.org/10.1111/j.1747-0285.2007.00483.x
14. Halgren TA. Identifying and Characterizing Binding Sites and Assessing Druggability. Journal of Chemical Information and Modeling [Internet]. American Chemical Society (ACS); 2009 Jan 20;49(2):377–89. Available from: http://dx.doi.org/10.1021/ci800324m
15. Friesner RA, Murphy RB, Repasky MP, Frye LL, Greenwood JR, Halgren TA, et al. Extra Precision Glide: Docking and Scoring Incorporating a Model of Hydrophobic Enclosure for Protein–Ligand Complexes. Journal of Medicinal Chemistry [Internet]. American Chemical Society (ACS); 2006 Sep 23;49(21):6177–96. Available from: http://dx.doi.org/10.1021/jm051256o
16. Li J, Abel R, Zhu K, Cao Y, Zhao S, Friesner RA. The VSGB 2.0 model: A next generation energy model for high resolution protein structure modeling. Proteins: Structure, Function, and Bioinformatics [Internet]. Wiley; 2011 Aug 22;79(10):2794–812. Available from: http://dx.doi.org/10.1002/prot.23106
17. Su P-C, Tsai C-C, Mehboob S, Hevener KE, Johnson ME. Comparison of radii sets, entropy, QM methods, and sampling on MM-PBSA, MM-GBSA, and QM/MM-GBSA ligand binding energies ofF. tularensisenoyl-ACP reductase (FabI). Journal of Computational Chemistry [Internet]. Wiley; 2015 Jul 27;36(25):1859–73. Available from: http://dx.doi.org/10.1002/jcc.24011
18. Bowers KJ, Sacerdoti FD, Salmon JK, Shan Y, Shaw DE, Chow E, et al. Molecular dynamics---Scalable algorithms for molecular dynamics simulations on commodity clusters. Proceedings of the 2006 ACM/IEEE conference on Supercomputing - SC '06 [Internet]. ACM Press; 2006; Available from: http://dx.doi.org/10.1145/1188455.1188544
19. Shekhar MS, Venkatachalam T, Sharma CS, Pratap Singh H, Kalra S, Kumar N. Computational investigation of binding mechanism of substituted pyrazinones targeting corticotropin releasing factor-1 receptor deliberated for anti-depressant drug design. Journal of Biomolecular Structure and Dynamics [Internet]. Informa UK Limited; 2018 Dec 24;37(12):3226–44. Available from: http://dx.doi.org/10.1080/07391102.2018.1513379
20. Benkert P, Biasini M, Schwede T. Toward the estimation of the absolute quality of individual protein structure models. Bioinformatics [Internet]. Oxford University Press (OUP); 2010 Dec 5;27(3):343–50. Available from: http://dx.doi.org/10.1093/bioinformatics/btq662
21. Patil R, Das S, Stanley A, Yadav L, Sudhakar A, Varma AK. Optimized Hydrophobic Interactions and Hydrogen Bonding at the Target-Ligand Interface Leads the Pathways of Drug-Designing. Hannenhalli S, editor. PLoS ONE [Internet]. Public Library of Science (PLoS); 2010 Aug 16;5(8):e12029. Available from: http://dx.doi.org/10.1371/journal.pone.0012029
22. Kumar H, Raj U, Gupta S, Varadwaj PK. In-silico identification of inhibitors against mutated BCR-ABL protein of chronic myeloid leukemia: a virtual screening and molecular dynamics simulation study. Journal of Biomolecular Structure and Dynamics [Internet]. Informa UK Limited; 2016 Jan 8;34(10):2171–83. Available from: http://dx.doi.org/10.1080/07391102.2015.1110046

HOW TO CITE THIS ARTICLE: Mishra SS, Sharma CS. Molecular Docking, Binding Energy and Molecular Dynamics Simulation Studies of Piperazin-1-ylpyridazine Derivatives as Deoxycytidine Triphosphate Pyrophosphatase Inhibitors. Int. J. Pharm. Sci. Drug Res. 2022;14(2):171-180. **DOI:** 10.25004/IJPSDR.2022.140203